ESTUDO DO EFEITO DA NANO-MODIFICAÇÃO DA MATRIZ NO ESTADO DE TENSÃO-DEFORMAÇÃO RESIDUAL DE PAINÉIS DE PLÁSTICO REFORÇADO COM FIBRA DE CARBONO

INVESTIGATION OF THE NANOSCALE MODIFICATION EFFECT OF MATRICES ON THE RESIDUAL STRESS-STRAIN STATE OF PLASTIC PANELS REINFORCED BY CARBON FIBERS

ИССЛЕДОВАНИЕ ВЛИЯНИЯ НАНОМОДИФИКАЦИИ МАТРИЦЫ НА ОСТАТОЧНОЕ НАПРЯЖЕННО-ДЕФОРМИРОВАННОГО СОСТОЯНИЕ ПАНЕЛЕЙ ИЗ УГЛЕПЛАСТИКА

KYAW, Aung Lin[1*]; RABINSKIY, Lev N.[2]

[1,2] Moscow Aviation Institute (National Research University), Department of Advanced Materials and Technologies of Aerospace Application, 4 Volokolamskoe highway, zip code 125993, Moscow – Russian Federation
(phone: +7 499 158-40-43)

** Corresponding author*
e-mail: kyawaung@mail.ru

Received 08 July 2018; received in revised form 30 November 2018; accepted 02 December 2018

RESUMO

O efeito da nano-modificação de plástico reforçado com fibra de carbono no estado de tensão-deformação residual após a moldagem foi investigado. Devido à alta anisotropia das propriedades físico-mecânicas, o resfriamento resulta em encolhimento das camadas do compósito irregular quanto às espessuras e direções. Isso leva a deflexões residuais e tensões internas nas peças compostas. No trabalho, uma técnica de estimação da influência de vários fatores físicos e mecânicos em estresses e tensões residuais foi desenvolvida. Com base nos dados obtidos, recomendações podem ser feitas para criar uma estrutura composta racional e métodos para reduzir tensões residuais e curvaturas. O principal fator que leva à ocorrência do estado de tensão-deformação residual é a anisotropia das propriedades da fibra de carbono, na qual as propriedades de rigidez e temperatura da camada unidirecional nas direções longitudinal e transversal diferem significativamente. Dependendo da estrutura da embalagem e das características dos componentes da monocamada (fibra e ligante), deformações lineares das camadas podem causar flexão do painel (flexão, torção) e o aparecimento de tensões térmicas residuais. São apresentados os resultados da modelagem analítica e numérica de deformações residuais em painéis com esquema de reforço assimétrico.

Palavras-chave: *fibra de carbono, nano-modificação, modelagem, deflexão, estado de tensão-deformação.*

ABSTRACT

The influence of nanomodification of carbon plastic on the residual stress-strain state (SSS) after molding has been studied. Due to the high anisotropy of the physical and mechanical properties, the non-uniform thickness and direction of shrinkage of the composite layers occur during cooling. This leads to the emergence of residual deflections and internal stresses in the composite parts. A method for estimating the influence of various physicomechanical factors on residual stresses and deformations has been developed. Based on the data obtained, recommendations can be made for the creation of a rational structure of the composite and methods for reducing residual stresses and curvatures. The main factor leading to the formation of residual SSS is the anisotropy of properties of carbon plastic, in which the rigidity and temperature properties of the unidirectional layer in the longitudinal and transverse directions are significantly different. Depending on the structure of the package and the characteristics of the components of the monolayer, linear deformation of the layers can cause panel curvature and to residual temperature stresses. The results of analytical and numerical modeling of residual deformations in panels with an asymmetric reinforcement scheme are presented.

DOI: 10.52571/PTQ.SI1.2018.164_PeriodicoES.pdf

Keywords: *carbon fiber, nanomodification, modeling, deflection, stress-strain state*.

АННОТАЦИЯ

Исследовано влияние наномодификации углепластика на остаточное напряженно-деформированное состояние (НДС) после формования. В силу высокой анизотропии физико-механических свойств при охлаждении происходит неравномерная по толщине и направлениям усадка слоев композита. Это приводит к появлению остаточных прогибов и внутренних напряжений в композитных деталях. В работе разработана методика оценки влияния различных физико-механических факторов на остаточные напряжения и деформации. На основе полученных данных могут быть составлены рекомендации по созданию рациональной структуры композита и методам снижения остаточных напряжений и кривизн. Основным фактором, приводящим к возникновению остаточного НДС, является анизотропия свойств углепластика, у которого жесткостные и температурные свойства однонаправленного слоя в продольном и поперечном направлениях значительно отличаются. В зависимости от структуры пакета и характеристик компонентов монослоя (волокна и связующего) линейные деформации слоев могут вызывать искривление панели (изгиб, крутку) и появление остаточных температурных напряжений. Представлены результаты аналитического и численного моделирования остаточных деформаций в панелях с несимметричной схемой армирования.

Ключевые слова: *углепластик, наномодификация, моделирование, прогиб, напряженно-деформированное состояние*.

INTRODUCTION

Nowadays, nanomodified carbon plastics are widely used in the aviation industry. Their use makes it possible to obtain a strong and rigid structure having a considerably smaller mass, as compared to a metal analog. In addition, the technology for creating complex products from nano-modified carbon fiber reinforced plastics is often cheaper and more practical due to the lack of many intermediate operations, which significantly reduces labor input and production costs. The possibility of changing the structure of carbon fiber makes it possible to maximize the use of the advantages of such materials and optimize the design for mass, rigidity and strength parameters (Budiman and Zuas, 2015).

One way to reduce residual stresses and deformations is nanomodification (Kuznetsova *et al.*, 2018; Kuznetsova *et al.*, 2015). The introduction of nanoscale particles in the composition of the composite or its components (fiber or binder) allows not only to increase its physical and mechanical properties but also to improve the residual stress-strain state. This problem has been discussed (Vasiliev *et al.*, 1990; Molodtsov *et al.*, 2000; Artemiev *et al.*, 2015; Dudchenko *et al.*, 2009; Zhuo *et al.*, 2017). A considerable number of works are devoted to the determination of residual deformations, the main of which are (Zhuo *et al.*, 2017; Lurie *et al.*, 2011; Astapov and Kornev, 2009; Afanasyev *et al.*, 1980; Blagonadezhin, 1995; Blagonadezhin and Indendaum, 1979; Kyung *et al.*, 2002; Lurie *et al.*, 2012).

The main task is to determine the degree of influence of the parameters of nanomodification on residual SSS. To this end, work was carried out to determine the residual SSS using the previously proposed model for the thermoelasticity of a layered composite. Effective physical and mechanical properties are determined on its basis (Malmeister et al., 1980; Nemirovsky, 1978; Sibgatullin and Sibgatullin, 2008; Tabanyukhova, 2012; Fedotov, 2012; Shaldyrvan, 1980; Yankovsky, 2012; Yankovsky, 2010).

Natural samples were fabricated, as well as elementary samples to experimentally determine the physicomechanical properties of the composite. To verify the data, the calculated and experimental deflections were compared.

MATERIALS AND METHODS

Consider a multi-layer panel made of a polymer composite having anisotropy due to the asymmetry of the properties of the packet structure over the thickness. The panel under consideration is free from load and fastening.

We introduce the coordinate system 1,2,3

(Figure 1), connected with the direction of the reinforcement. For unidirectional material, the axis 1 is aligned with the direction of the fibers, for the woven – the axis 1 coincides with the direction of the warp thread. Axis 2 is perpendicular to the axis 1 and lies in the reinforcement plane. The axis 3 is directed along the thickness of the layer and is orthogonal to the plane of the layer. For the panel, we introduce the coordinate system x, y, z so that the x, y-axes lie in the reinforcement plane, and the z-axis is directed along the thickness of the packet.

In the general case, six internal force factors appear in the panel: N x, N y, N x y, M x , M y , M x y (Figure 2).

The physical relationships, in this case, will have the following form Equation 1. Where $N_x^T, N_y^T, N_{xy}^T, N_x^н, N_y^н, N_{xy}^н$ – linear forces caused by temperature deformation (index *T*) and initial tension of layers (index *n*); $M_x^T, M_y^T, M_{xy}^T, M_x^н, M_y^н, M_{xy}^н$ – linear moments caused by temperature deformation (index *T*) and initial tension of layers (index *n*); B_{mn}, C_{mn}, D_{mn} – generalized rigidity of the packet (*m, n* = 1,2,3); $e_x, e_y e_{xy}$ – linear deformation of the packet in the reduction plane; $k_x, k_y k_{xy}$ – the curvature of the packet in the reduction plane. Let's write down the relationship of the deformation of the panel in the reduction plane with displacements u_0, v_0 (Equation 2). The relationship between the curvature of the panel and the angles of rotation of the normal θ_x, θ_y (Equation 3). The relationship of the angles of rotation of the normal to the deflection *w* is as follows (Equation 4), where γ_{xz} -, γ_{yz}- transverse shear. The generalized stiffnesses of a packet are defined as follows (Equations 5 – 7). Where *e* is the coordinate of the reduction plane (for an asymmetric packet it is chosen arbitrarily); *m, n* = 1,2,3 , *r* = 0,1,2. Let's write the expressions for the forces and moments caused by the temperature fields (Equations 8, 9). Where (Equations 10, 11) Z_k is the coordinate of the *k*-th layer, reckoned from the reduction plane; *N* is the number of layers; $b_{ij}^{(k)}$ - linear stiffnesses of the *k*- th layer, reduced to the axes of the panel (x, *y*) (*i, j* = 1, 2, 3); ΔT - temperature drop due to cooling; $\overline{a}_1^{(k)}, \overline{a}_2^{(k)}, \overline{a}_3^{(k)}$ – coefficients of linear thermal expansion of the *k*- th layer in the axes of the panel; Similarly, we record the forces and moments from the initial tension (Equations 12, 13). Where (Equations 14, 15) $\overline{\varepsilon}_{н1}^{(k)}, \overline{\varepsilon}_{н2}^{(k)}, \overline{\varepsilon}_{н3}^{(k)}$ – initial deformation of the layers in the axes of the panel. Linear rigidity for the *k*- th layer in the case of an asymmetric packet has the following form Equations 16, 17. The factor of linear temperature expansion for the *k*- th layer, as well as deformation of the layer, caused by the initial tension, in the axes of the panel, are determined by the appropriate transformation (Equations 18, 19). In the above formulas, $m^{(k)}$ and $n^{(k)}$ – are trigonometric functions of the angle of orientation of the layers $\varphi^{(k)}$ with respect to the *x*-axis of the panel represented in the Equation 20.

We shall consider a flat panel without initial curvature with edges free from loading and fixation, subject to the action of a temperature field uniformly distributed over the thickness. The actuating surface coincides with the average surface. For the orthotropic structure of a composite $B_{13} = B_{31} = 0$, and the coefficients $C_{13}, C_{31}, C_{23}, C_{32}, D_{13}, D_{31}$ are small and they can be neglected. Taking this into account, the physical relationships for the orthotropic structure of the composite in expanded form will take the form (Equations 21,22). Thus, it is easy to see that in the case of the orthotropic structure of the composite material, the definition of the deformed state is divided into 2 independent problems of finding deflections (the components of curvature κ_x, κ_y) and twist (κ_{xy}). The stresses in the layers are determined from Hooke's law, using the components of curvature and deformation obtained from (Equation 1), ie (Equation 23). In this case, z_k is the coordinate of the middle surface of the layer, that is, $z_k = (Z_k - e) - h_k / 2$.

For the transition to stress σ_1, σ_2, τ_{12} in the axes of the layer, it is necessary to use the transformation formulas for the rotation of the coordinate axes (Equation 24). As we can see from the physical relationships (1) in multilayer panels with asymmetrical packing, the layers subject to tension-compression will cause the panel to bend. Such complex behavior of panels in the structure of highly loaded structures can lead to a decrease in the efficiency of their

operation.

In addition, the molding of such panels will be accompanied by the appearance of residual thermal bending deformations (warpage).

This disadvantage is absent in a panel with a symmetrical arrangement of layers, i.e. when the layer (*k*) corresponds to the same layer (*Nk*), where *N is the* total number of layers in the packet. Taking this into account, let's write down the expressions for generalized rigidities in the following simplified form Equation 25. The coordinate $Z_{k\,is}$ then counted from the mid-plane $e = h / 2$, and the sum is calculated only for half the packet. The physical relationships (1) for an orthotropic panel with load-free edges take the following form Equations 26, 27.

From Equation 21 it is easy to see that forming flat panels with a symmetrical structure of the packet will not lead to their warping.

The algorithm for analyzing the residual stress-strain state can thus be divided into four stages:

1) calculation of the stiffness characteristics of the packet according to Equations 5, 6,15 –19;

2) determination of internal force factors caused by initial tension and temperature drop according to formulas Equations 9 – 13;

3) definition of components of deformations and curvature of physical relationships Equation 1;

4) calculation of stresses in the layers of the composite with the help of Hooke's law Equations 23, 24.

RESULTS AND DISCUSSION:

For the analytical calculation: the plate is free from fastening and external power load, the temperature load is a drop of 100 °C. For the finite element calculation: the plate is fixed at the geometrical center of load, the temperature load – a difference of about 100 °C. The characteristics of materials used in modeling are presented in Table 1. Two variants of laying the composite were considered (Table 2 and Table 3). For each variant of laying, four calculations were carried out using the properties of the carbon plastimonolayer from Table 1.

Similarly, 4 calculations were carried out using the properties of a monolayer of nanomodified carbon fiber reinforced plastics from Table 1.

Total calculations conducted to 8 for styling embodiment [0 10/45 $_{10}$] and 8 calculations – for [0 10/90 10].

Different stacking layers are given in Tables 2-3

The produced plates were measured along the deflections along each of the four sides. For this, two extreme points were fixed on an even surface, the deflection was measured in the center of the side by a caliper. The results of the calculations performed with different stacking options are given in Tables 4-5 An illustration of these calculations for various types of packing is shown in Figures 3-4

CONCLUSIONS:

In this paper, the authors propose a technique for calculating the residual stresses and deformations of flat panels made from nanomodified carbon plastics. To calculate the effective properties of a monolayer, taking into account the influence of the parameters of whiskerizing, an approach based on solving the problem of multilayer cylindrical inclusion was used. The properties of the interphase zone were determined on the basis of a model of elliptic chaotically oriented inclusions. The residual stresses in the panel were determined using the classical model of thermoelasticity of layered composites. As an example, the problem of determining residual stresses, deformations and curvatures in a carbon plastic plate reinforced with viscous fibers, on the surface of which carbon nanotubes were grown, was considered. The performed calculations show the possibility, in practice, of completely eliminating residual stresses and deformations in materials with different reinforcement schemes. It is shown that, based on the proposed model, it is possible to predict optimal variants of whiskerizing, which allows lowering the anisotropy of the coefficients of temperature expansion of the composite. The results obtained by analytical and numerical methods are identical. The greatest similarity with the experimental data is provided by method 4 in determining the effective properties of a monolayer.

ACKNOWLEDGMENTS:

This work was supported by the Russian Science Foundation under grant 17-79-20105 issued to the Moscow Aviation Institute.

REFERENCES:

1. Afanasyev, Yu.A., Ekelchik, B.C., Kostritsky, S.N. *Mechanics of Composite Materials*, **1980**, *4*, 651-660.
2. Artemiev, A.V., Afanasiev, A.V., Rabinskiy, L.N., Lin, J.A. *Nanomechanics Science and Technology: An International Journal*, **2015**, *6(4)*, 251-260.
3. Astapov, N.S., Kornev, V.M. *Mechanics of composite materials and structures*, **2009**, *15(3)*, 307 318.
4. Blagonadezhin, V.A., Indendaum, V.M. *Strength Calculations*, **1979**, *20*, 209-228.
5. Blagonadezhin, V.L. *Mechanics of Polymers*, **1975**, *6*, 996-1004.
6. Budiman, H., Zuas, O. *Periodico Tche Quimica*, **2015**, *12(24)*, 7-16
7. Dudchenko, AA, Lurie, S.A., Shumova, N.P. *Bulletin of the Moscow Aviation Institute*, **2009**, *16(5)*, 144-148.
8. Fedotov, A.F. *Mechanics of Composite Materials and Structures*, **2012**, *18(4)*, 508-526.
9. Kuznetsova, E.L., Kuznetsova, E.L., Rabinskiy, L.N., Zhavoronok, S.I. *Journal of Vibroengineering*, **2018**, *20(2)*, 1108-1117
10. Kuznetsova, E.L., Leonenko, D.V., Starovoitov, E.I. *Mechanics of Solids*, **2015**, *50(3), A012*, 359-366
11. Kyung, Le Kim, Lurie, S.A., Dudchenko, A.A. *Mechanics of Composite Materials and Structures*, **2012**, *18(1)*, 83 -91.
12. Lurie, S.A., Belov, P.A., Rabinsky, L.N., Zhavoronok, S.I. *Large-scale effects in the mechanics of continuous media. Materials from micro-and nanostructures*, Moscow: MAI, **2011**.
13. Lurie, SA, Fam, T., Solyayev, Yu.O. *Mechanics of Composite Materials and Structures*, **2012**, *18(3)*, 440 449.
14. Malmeister, A.K., Tamuzh, V.P., Teter, G.A. *Resistance of polymer and composite materials*, Riga: Zinatne, **1980**.
15. Molodtsov, G.A., Bitkin, V.E., Simonov, V.F., Urmansov, F.F. *Formostable and intelligent structures made of composite materials*, Moscow: Mashinostroyeniye, **2000**.
16. Nemirovsky, Yu.V. *Mechanics of Polymers*, **1978**, *4*, 675-682.
17. Shaldyrvan, V.A. *Mechanics of Composite Materials and Structures*, **1980**, *33(2)*, 55-63.
18. Sibgatullin, E.S., Sibgatullin, K.E. *Mechanics of Composite Materials and Structures*, **2008**, *14(4)*, 572-582.
19. Tabanyukhova, M. *Mechanics of Composite Materials and Structures*, **2012**, *18(2)*, 248-254.
20. Vasiliev, V.V., Protasov, V.D., Bolotin, V.V. *Composite materials*, Moscow: Mashinostroyeniye, **1990**.
21. Yankovsky, A.P. *Constructions from Composite Materials*, **2012**, *2*, 12-25.
22. Yankovsky, A.P. *Mechanics of Composite Materials,* **2010**, *46(5)*, 663 678.
23. Zhuo, AL, Artemiev, AV, Afanasyev, AV, Rabinsky, LN, Semenov, NA, Solyayev, Yu.O. *Bulletin of the Moscow Aviation Institute*, **2017**, *24(2)*, 197-208.

$$\begin{pmatrix} N_x \\ N_y \\ N_{xy} \\ M_x \\ M_y \\ M_{xy} \end{pmatrix} = \begin{pmatrix} B_{11} & B_{12} & B_{13} & C_{11} & C_{12} & C_{13} \\ B_{21} & B_{22} & B_{23} & C_{21} & C_{22} & C_{23} \\ B_{31} & B_{32} & B_{33} & C_{31} & C_{32} & C_{33} \\ C_{11} & C_{12} & C_{13} & D_{11} & D_{12} & D_{13} \\ C_{21} & C_{22} & C_{23} & D_{21} & D_{22} & D_{23} \\ C_{31} & C_{32} & C_{33} & D_{31} & D_{32} & D_{33} \end{pmatrix} \times \begin{pmatrix} \varepsilon_x \\ \varepsilon_y \\ \varepsilon_{xy} \\ \kappa_x \\ \kappa_y \\ \kappa_{xy} \end{pmatrix} - \begin{pmatrix} N_x{}^T \\ N_y{}^T \\ N_{xy}{}^T \\ M_x{}^T \\ M_y{}^T \\ M_{xy}{}^T \end{pmatrix} - \begin{pmatrix} N_x{}^н \\ N_y{}^н \\ N_{xy}{}^н \\ M_x{}^н \\ M_y{}^н \\ M_{xy}{}^н \end{pmatrix}. \quad (1)$$

$$\varepsilon_x = \frac{\partial u_0}{\partial x}; \varepsilon_y = \frac{\partial v_0}{\partial y}; \varepsilon_{xy} = \frac{\partial u_0}{\partial y} + \frac{\partial v_0}{\partial x}. \quad (2)$$

$$\kappa_x = \frac{\partial \theta_x}{\partial x}; \kappa_y = \frac{\partial \theta_y}{\partial y}; \kappa_{xy} = \frac{\partial \theta_x}{\partial y} + \frac{\partial \theta_y}{\partial x}. \quad (3)$$

$$\theta_x = \psi_x - \frac{\partial w}{\partial x}; \theta_y = \psi_y - \frac{\partial w}{\partial y}, \quad (4)$$

$$B_{mn} = I^{(0)}{}_{mn}, \quad (5)$$

$$D_{mn} = I^{(2)}{}_{mn} - 2eI^{(1)}{}_{mn} + e^2 I^{(0)}{}_{mn}, . \quad (6)$$

$$I^{(r)}{}_{mn} = \int_0^h b_{mn} Z^r dt = \frac{1}{r+1} \sum_{k=1}^{N} b_{mn}^{(k)} (Z_k{}^{r+1} - Z_{k-1}{}^{r+1}), \quad (7)$$

$$N_x{}^T = \sum_{j=1}^{3} N_{1j}^T, N_y{}^T = \sum_{j=1}^{3} N_{2j}^T, N_{xy}{}^T = \sum_{j=1}^{3} N_{3j}^T, \quad (8)$$

$$M_x{}^T = \sum_{j=1}^{3} M_{1j}^T, M_y{}^T = \sum_{j=1}^{3} M_{2j}^T, M_{xy}{}^T = \sum_{j=1}^{3} M_{3j}^T, \quad (9)$$

$$N_{ij}^T = \Delta T \sum_{k=1}^{N} [b_{ij}{}^{(k)} \overline{\alpha_j^{(k)}} (Z_k - Z_{k-1})]; \quad (10)$$

$$M_{ij}^T = \Delta T \sum_{k=1}^{N} b_{ij}{}^{(k)} \overline{\alpha_j^{(k)}} \left[\frac{1}{2} (Z_k{}^2 - Z_{k-1}{}^2) - e(Z_k - Z_{k-1}) \right]; \quad (11)$$

$$N_x{}^н = \sum_{j=1}^{3} N_{1j}^н, N_y{}^н = \sum_{j=1}^{3} N_{2j}^н, N_{xy}{}^н = \sum_{j=1}^{3} N_{3j}^н, \quad (12)$$

$$M_x^{н} = \sum_{j=1}^{3} M_{1j}^{н}, M_y^{н} = \sum_{j=1}^{3} M_{2j}^{н}, M_{xy}^{н} = \sum_{j=1}^{3} M_{3j}^{н}, . \quad (13)$$

$$N_{ij}^{н} = \sum_{k=1}^{N} [b_{ij}^{(k)} \overline{\varepsilon_{нj}^{(k)}} (Z_k - Z_{k-1})]; \quad (14)$$

$$M_{ij}^{н} = \sum_{k=1}^{N} b_{ij}^{(k)} \overline{\varepsilon_{нj}^{(k)}} \left[\frac{1}{2} (Z_k^{\,2} - Z_{k-1}^{\,2}) - e(Z_k - Z_{k-1}) \right]; \quad (15)$$

$$\begin{aligned}
b_{11}^{(k)} &= [\overline{E_1} m^4 + \overline{E_2} n^4 + 2(\overline{E_1} \nu_{12} + 2G_{12}) m^2 n^2]^{(k)} \\
b_{22}^{(k)} &= [\overline{E_1} n^4 + \overline{E_2} m^4 + 2(\overline{E_1} \nu_{12} + 2G_{12}) m^2 n^2]^{(k)} \\
b_{12}^{(k)} &= b_{21}^{(k)} = \left[\overline{E_1} \nu_{12} + [\overline{E_1} + \overline{E_2} - 2(\overline{E_1} \nu_{12} + 2G_{12})] m^2 n^2 \right]^{(k)} \\
b_{13}^{(k)} &= b_{31}^{(k)} = \left[mn \left[\overline{E_1} m^2 - \overline{E_2} n^2 - \left(\overline{E_1} \nu_{12} + 2G_{12} \right) \left(m^2 - n^2 \right) \right] \right]^{(k)}, \\
b_{23}^{(k)} &= b_{32}^{(k)} = \left[mn \left[\overline{E_1} n^2 - \overline{E_2} m^2 + \left(\overline{E_1} \nu_{12} + 2G_{12} \right) \left(m^2 - n^2 \right) \right] \right]^{(k)} \\
b_{33}^{(k)} &= [(\overline{E_1} + \overline{E_2} - 2\overline{E_1} \nu_{12}) m^2 n^2 + G_{12} (m^2 - n^2)]^{(k)}
\end{aligned} \quad (16)$$

$$\begin{aligned}
E_1^{(k)} &= \frac{E_1^{(k)}}{1 - \nu_{12}^{(k)} \nu_{21}^{(k)}}, \\
E_2^{(k)} &= \frac{E_2^{(k)}}{1 - \nu_{12}^{(k)} \nu_{21}^{(k)}}, .
\end{aligned} \quad (17)$$

$$\begin{pmatrix} \overline{\alpha_1} \\ \overline{\alpha_2} \\ \overline{\alpha_3} \end{pmatrix}^{(k)} = \begin{pmatrix} m^2 & n^2 \\ n^2 & m^2 \\ 2mn & -2mn \end{pmatrix}^{(k)} \begin{pmatrix} \alpha_1 \\ \alpha_2 \end{pmatrix}^{(k)}, \quad (18)$$

$$\begin{pmatrix} \overline{\varepsilon_{н1}} \\ \overline{\varepsilon_{н2}} \\ \overline{\varepsilon_{н3}} \end{pmatrix}^{(k)} = \begin{pmatrix} m^2 \\ n^2 \\ 2mn \end{pmatrix}^{(k)} (\varepsilon_{н})^{(k)}. \quad (19)$$

$$\begin{aligned}
m^{(k)} &= \cos(\varphi^{(k)}), \\
n^{(k)} &= \sin(\varphi^{(k)}). \quad .
\end{aligned} \quad (20)$$

$$\begin{cases} 0 = B_{11}\varepsilon_x + B_{12}\varepsilon_y + C_{11}\kappa_x + C_{12}\kappa_y - N_x^{\ T} - N_x^{\ н} \\ 0 = B_{12}\varepsilon_x + B_{22}\varepsilon_y + C_{21}\kappa_x + C_{22}\kappa_y - N_y^{\ T} - N_y^{\ н} \\ 0 = C_{11}\varepsilon_x + C_{12}\varepsilon_y + D_{11}\kappa_x + D_{12}\kappa_y - M_x^{\ T} - M_x^{\ н} \\ 0 = C_{21}\varepsilon_x + C_{22}\varepsilon_y + D_{21}\kappa_x + D_{22}\kappa_y - M_y^{\ T} - M_y^{\ н} \end{cases}. \quad (21)$$

$$\begin{cases} 0 = B_{33}\varepsilon_{xy} + C_{33}\kappa_{xy} - N_{xy}^{\ T} - N_{xy}^{\ н} \\ 0 = C_{33}\varepsilon_{xy} + D_{33}\kappa_{xy} - M_{xy}^{\ T} - M_{xy} \end{cases} \quad (22)$$

$$\begin{pmatrix} \sigma_x \\ \sigma_y \\ \tau_{xy} \end{pmatrix}^{(k)} = \begin{pmatrix} b_{11} & b_{12} & b_{13} \\ b_{21} & b_{22} & b_{23} \\ b_{31} & b_{32} & b_{33} \end{pmatrix}^{(k)} \begin{pmatrix} \varepsilon_x + \kappa_x \cdot z_k - \overline{\alpha_1}^{(k)} \cdot \Delta T - \overline{\varepsilon_{н1}}^{(k)} \\ \varepsilon_y + \kappa_y \cdot z_k - \overline{\alpha_2}^{(k)} \cdot \Delta T - \overline{\varepsilon_{н2}}^{(k)} \\ \varepsilon_{xy} + \kappa_{xy} \cdot z_k - \overline{\alpha_3}^{(k)} \cdot \Delta T - \overline{\varepsilon_{н3}}^{(k)} \end{pmatrix}. \quad (23)$$

$$\begin{pmatrix} \sigma_1 \\ \sigma_2 \\ \tau_{12} \end{pmatrix}^{(k)} = \begin{pmatrix} m^2 & n^2 & 2mn \\ n^2 & m^2 & -2mn \\ -mn & mn & (m^2 - n^2) \end{pmatrix}^{(k)} \begin{pmatrix} \sigma_x \\ \sigma_y \\ \tau_{xy} \end{pmatrix}^{(k)}. \quad (24)$$

$$\begin{aligned} B_{mn} &= 2\sum_{k=1}^{N/2} b_{mn}^{\ (k)} (Z_k - Z_{k-1}) \\ D_{mn} &= \frac{2}{3}\sum_{k=1}^{N/2} b_{mn}^{\ (k)} (Z_k^{\ 3} - Z_{k-1}^{\ 3}) \\ C_{mn} &= 0 \end{aligned} \quad (25)$$

$$\begin{cases} 0 = B_{11}\varepsilon_x + B_{12}\varepsilon_y - N_x^{\ t} - N_x^{\ н} \\ 0 = B_{12}\varepsilon_x + B_{22}\varepsilon_y - N_y^{\ t} - N_y^{\ н} \\ 0 = D_{11}\kappa_x + D_{12}\kappa_y \\ 0 = D_{21}\kappa_x + D_{22}\kappa_y \end{cases} \quad (26)$$

$$\begin{cases} 0 = B_{33}\varepsilon_{xy} - N_{xy}^{\ t} - N_{xy}^{\ н} \\ 0 = D_{33}\kappa_{xy} \end{cases}. \quad (27)$$

Table 1. *Physical and mechanical characteristics of materials*

No.		E_{11} [MPa]	E_{22} [MPa]	G_{12} [MPa]	ν_{12}	α_1 [10^{-6} K^{-1}]	α_2, α_3 [10^{-6} K^{-1}]	G_{23} [MPa]
1	Carbon plastic	129960	7056	2658	0.593	0.7	42	2214
	Nanomodified carbon plastic	135130	19078	8225	0.567	3.4.	44	6085
2	Carbon plastic	129510	5211	1917	0.596	0.46	42	1632
	Nanomodified carbon plastic	129760	6266	2337	0.594	0.6	42	1965
3	Carbon plastic	129500	4730	2050	0.29	0.19	20	1670
	Nanomodified carbon plastic	129750	5700	2500	0.29	0.26	20	2010
4	Carbon plastic	129500	4730	2050	0.29	-10.4	20	1670
	Nanomodified carbon plastic	129750	5700	2500	0.29	-12	20	2010

Table 2. *Stacking of layers [0 10/45 10]*

No.	Material	Number of layers	Angle, degrees	Layer thickness, mm
1	Carbon plastic	10	0	0.2
2	Carbon plastic	10	45	0.2
Total thickness:				*4.1*

Table 3. *Stacking of layers [0 10/90 10]*

No.	Material	Number of layers	Angle, degrees	Layer thickness, mm
1	Carbon plastic	10	0	0.2
2	Carbon plastic	10	90	0.2
Total thickness:				*4.1*

Table 4. *Comparison of deflections for options 1-4 and laying [0 10/45 $_{10}$] with experiment*

		1	2	3	4	Experiment
Deflection on the long side, mm	With nano	10.6	6.6	3.2	5.1	**4.35**
	Without nano	7	5.3	2.8	4.3	**3.2**
Deflection on the short side, mm	With nano	5.7	3.5	1.7	2.8	**2.1**
	Without nano	3.8	2.8	1.5	2.3	**2.75**

Table 5. *Comparison of deflections for options 1-4 and laying [0 10/90 $_{10}$] with experiment*

		1	2	3	4	Experiment
Deflection on the long side, mm	With nano	19.9	12.4	5.6	9.2	**5.85**
	Without nano	13.3	10	5	7.7	**5.95**
Deflection on the short side, mm	With nano	10.7	6.7	3	4.9	**4.1**
	Without nano	7.2	5.4	2.7	4.2	**3.7**

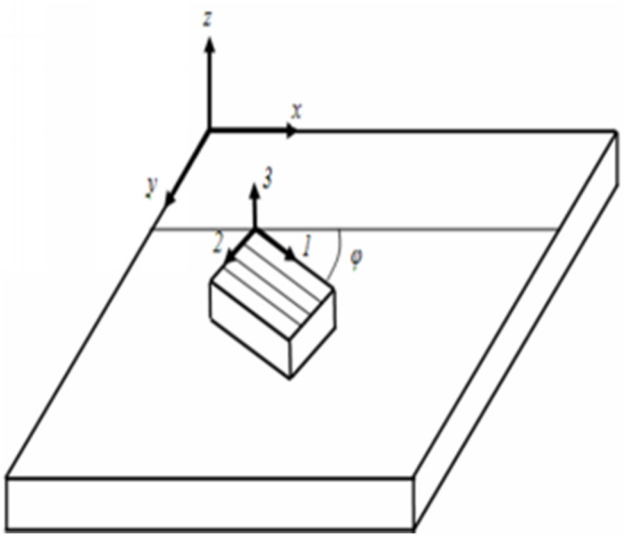

Figure 1. *Layer and panel coordinate systems*

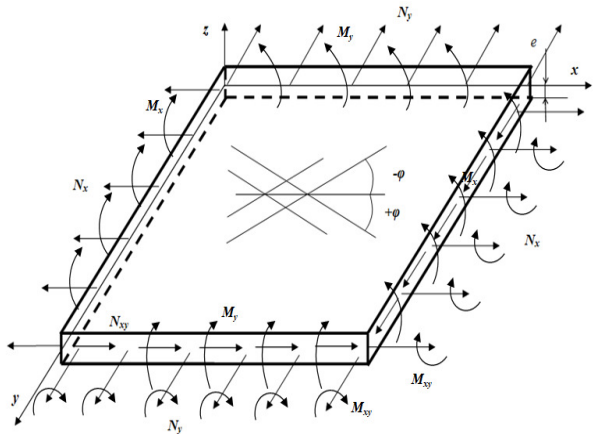

Figure 2. *The geometric model and the emerging internal force factors of a plate with an asymmetric packet structure*

Without nano *With nano*

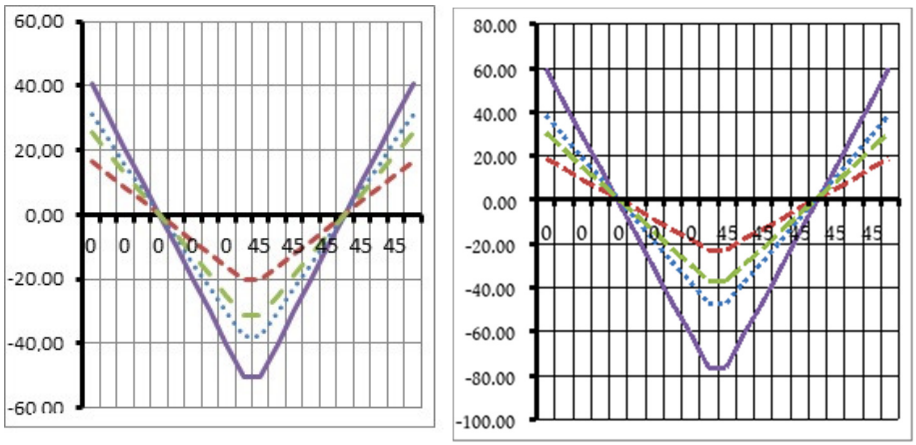

Distribution of normal stresses over the layers σ_1*, MPa*

With nano *Without nano*

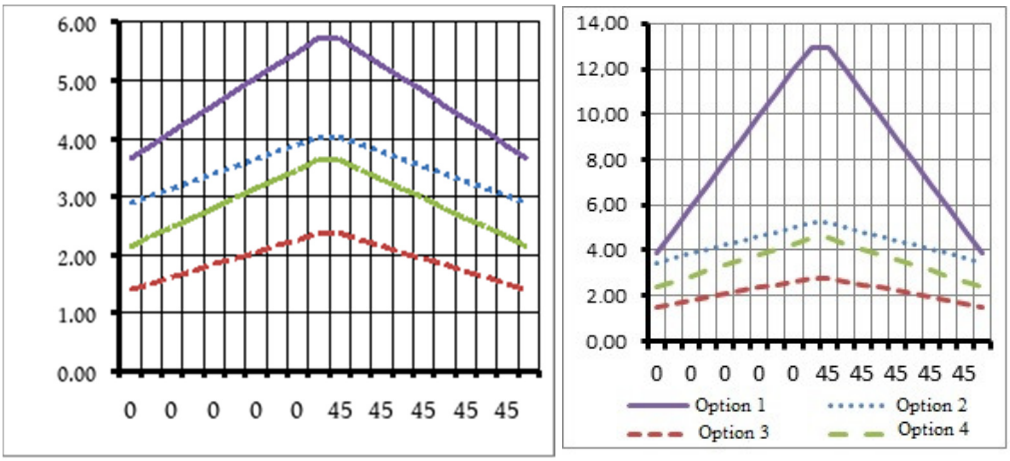

The distribution of normal stresses over the layers σ_2*, MPa*

Without nano *With nano*

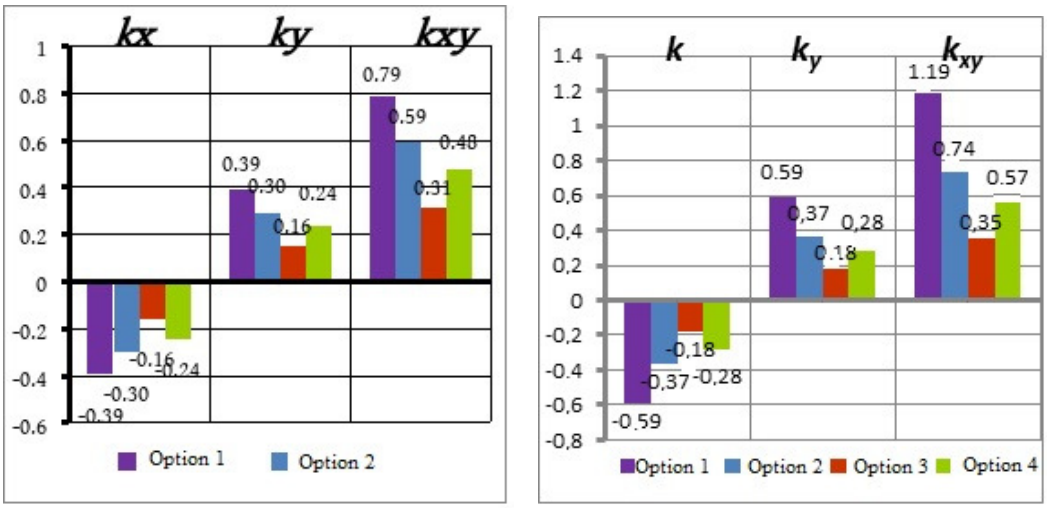

The values of the components of curvature

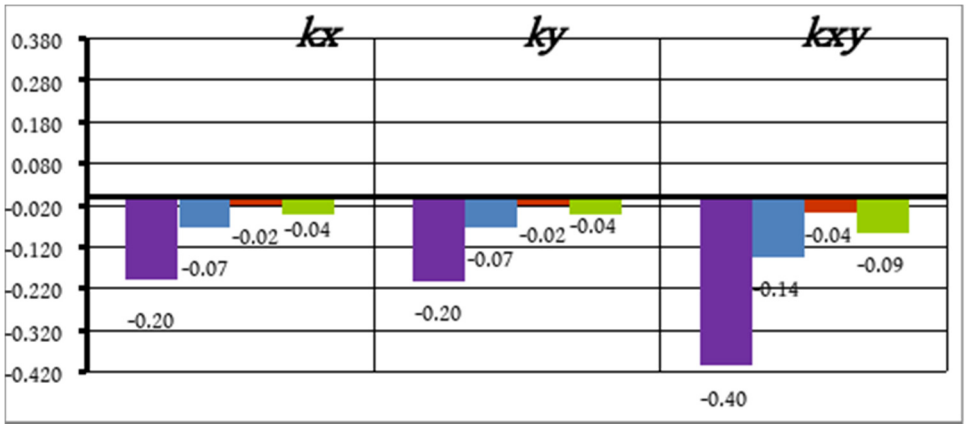

The difference between the components of curvature for carbon plastic with nanomodification and without

Figure 3. *Summary table of the results for options 1-4 and laying [0 10/45 10]*

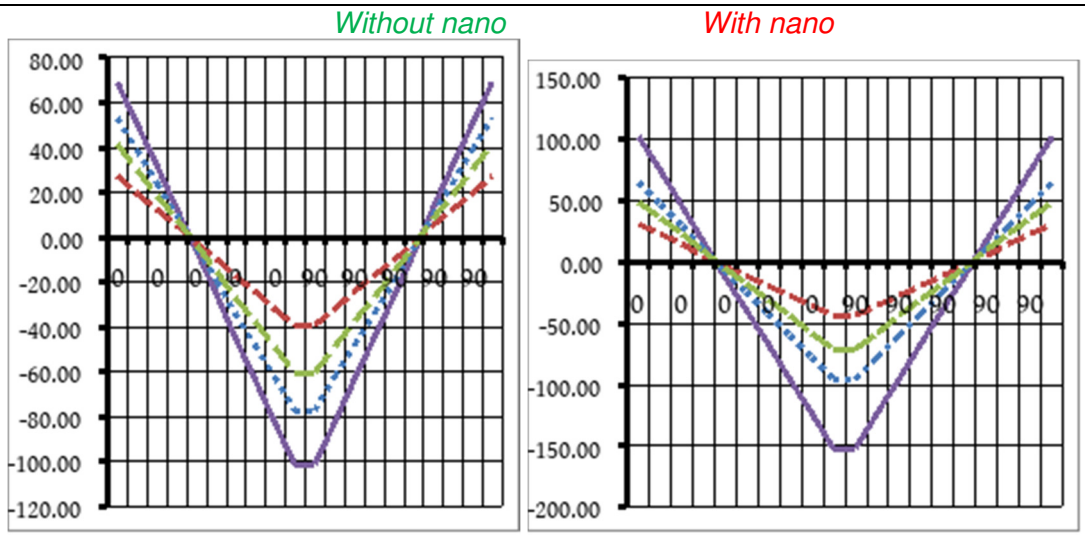

Distribution of normal stresses over the layers σ_1*, MPa*

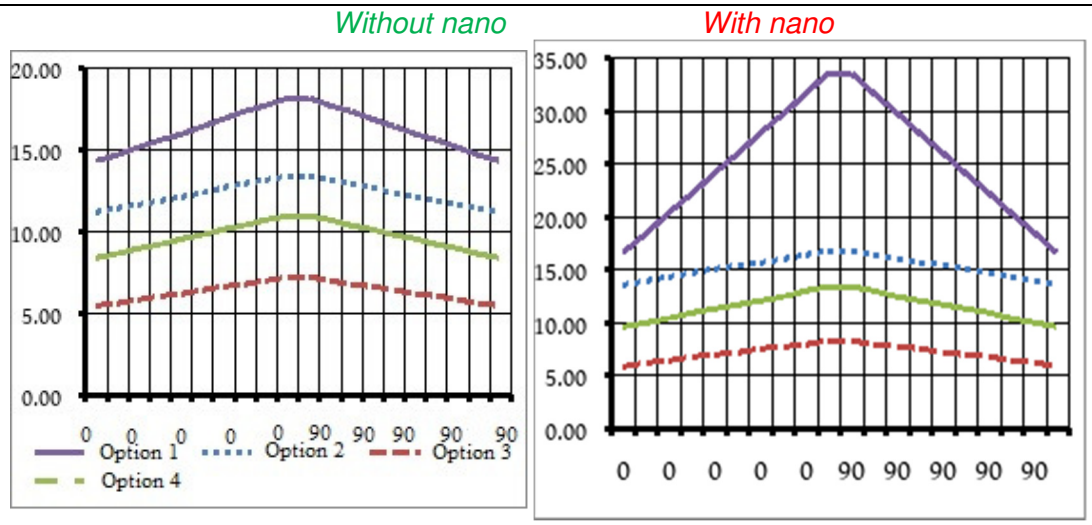

The distribution of normal stresses over the layers σ_2*, MPa*

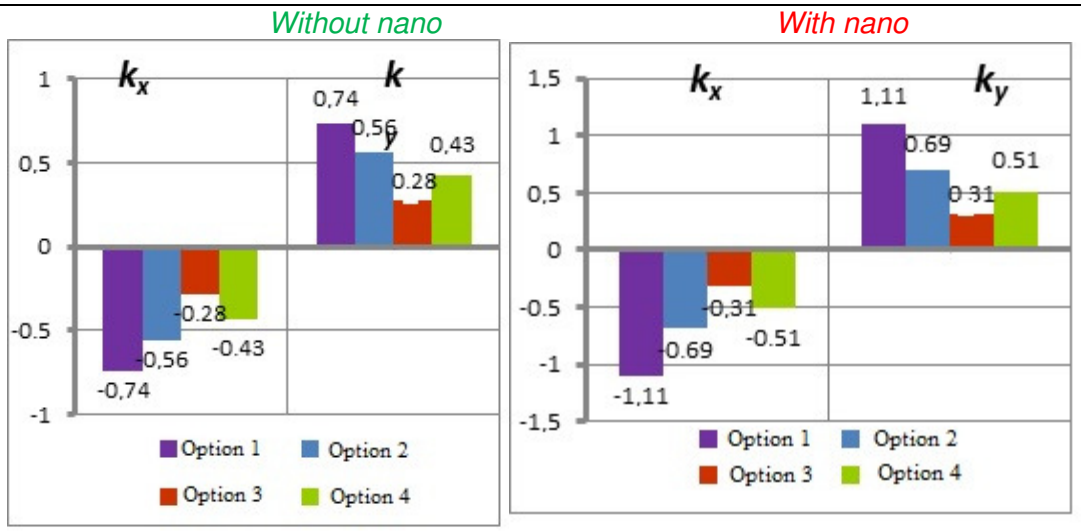

The values of the components of curvature

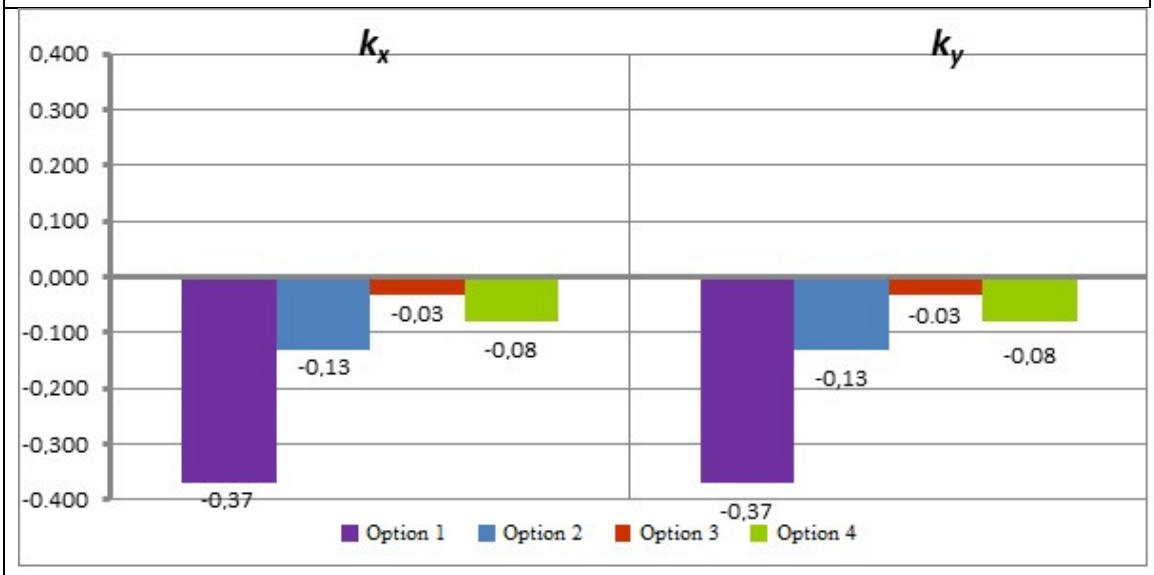

Without nano *With nano*

The difference between the components of curvature for carbon plastic with nanomodification and without

Figure 4. *Summary table of the results for options 1-4 and laying [0 10/90 10]*